Magnetic and structural properties of erbium films

G. Helgesen
Institute for Energy Technology, N-2007 Kjeller, Norway
and Brookhaven National Laboratory, Upton, New York 11973

Y. Tanaka
The Institute of Physical and Chemical Research (RIKEN), Wako, Saitama 351-01, Japan

J. P. Hill, P. Wochner, and Doon Gibbs
Brookhaven National Laboratory, Upton, New York 11973

C. P. Flynn and M. B. Salamon
Department of Physics, University of Illinois at Urbana-Champaign, Urbana, Illinois 61801
(Received 3 February 1997)

The results of x-ray-scattering studies of the magnetic and structural properties of two erbium thin films (thickness$\geqslant$1 μm) grown epitaxially on Lu and Y substrates are presented. These substrates, respectively, compress or expand the erbium a-axis lattice constants and clamp them at the film-substrate interfaces, thereby introducing epitaxial strain. Detailed measurements of the temperature dependence of the c- and a-axis lattice constants, magnetic wave vectors, and magnetic order parameters of the films are reported. The qualitative features of the magnetic phase behavior mirror those of the bulk, including the scaling of the order-parameter critical exponents β_n and the existence of lock-in transitions to bulk commensurate wave vectors. The magnetic phase transitions, however, exhibit marked hysteresis and the magnetic structures are characterized by multiphase coexistence and limited correlation lengths. The low-temperature phase of bulk erbium with magnetic wave vector 5/21 is suppressed in both films, and is replaced in Er/Lu by two new phases with wave vectors near 6/25 and 11/45. Qualitative c-axis strain profiles are deduced from the measurements and confirm that the Er/Y film is more distorted than the Er/Lu. [S0163-1829(97)04630-4]

I. INTRODUCTION

In recent years, neutron and x-ray-scattering studies of thin rare-earth films and multilayers have revealed a rich complex of magnetic phases which could not have been predicted from the behavior of the pure, bulk magnetic systems.[1] As is well known, magnetic ordering in the rare-earth metals stems from the competition among two-ion indirect exchange interactions between localized moments of the $4f$ electrons (the RKKY interaction) and anisotropic single-ion crystal-field interactions.[2–4] In the magnetically ordered phases, magnetoelastic interactions may modify the balance, further altering the magnetic phase diagrams. In thin films and multilayers the picture is made even more complicated due to the lattice strain and clamping originating at the layer interfaces. The purpose of the present work was to utilize high-resolution x-ray diffraction to characterize these latter processes in two otherwise similar erbium films grown epitaxially on different substrates. The first sample was an Er film grown on a Lu substrate,[5] which gives rise on average to a compressional strain in the basal plane of the film and a corresponding expansion along its c axis. The second sample was grown on a Y substrate,[6] which leads to in-plane expansion relative to bulk Er and a contraction along the c axis. This is illustrated in Fig. 1.

Briefly, we have found that the qualitative features of the magnetic phase diagrams of the films are similar to those occurring in bulk. For example, both films order at $T_N \approx 86$ K into c-axis modulated structures with the same wave vectors as does bulk Er. However, the epitaxial strain and clamping imposed at the film-substrate interfaces alters the detailed temperature dependence of the magnetic structures, most notably by the introduction of multiphase coexistence, by suppression of the 5/21 phase at low temperature and by marked hysteresis at the magnetic phase transitions. Moreover, while the crystal symmetries of the films remain unchanged from bulk Er, the lattice and magnetic correlation lengths are reduced, consistent with a high degree of disorder. Indeed, in the low-temperature phase of Er/Y, we find that the magnetic correlation lengths are comparable to the unit-cell size of the magnetic structures. In Er/Lu below 20 K, two new magnetic wave vectors falling between 5/21 and 1/4 were observed. They probably correspond to conical phases similar to the bulk 5/21 phase. Detailed measurements of the temperature dependence of the first- and second-order satellite peaks near T_N show that the order-parameter critical exponent $\beta \approx 1/2$ in both films, and that the amplitude of the higher harmonics satisfies mean-field scaling, consistent with bulk erbium.[7] While the magnetic phase behavior of the films may still be considered within the physics of competing interactions, coupling the exchange, crystal-field, and magnetoelastic contributions, as in the bulk, in the films the underlying lattice is disordered, which we believe introduces disorder into the coupling. This disorder may play a significant role in the resulting magnetic order. These kinds of effects are usually considered within the context of the

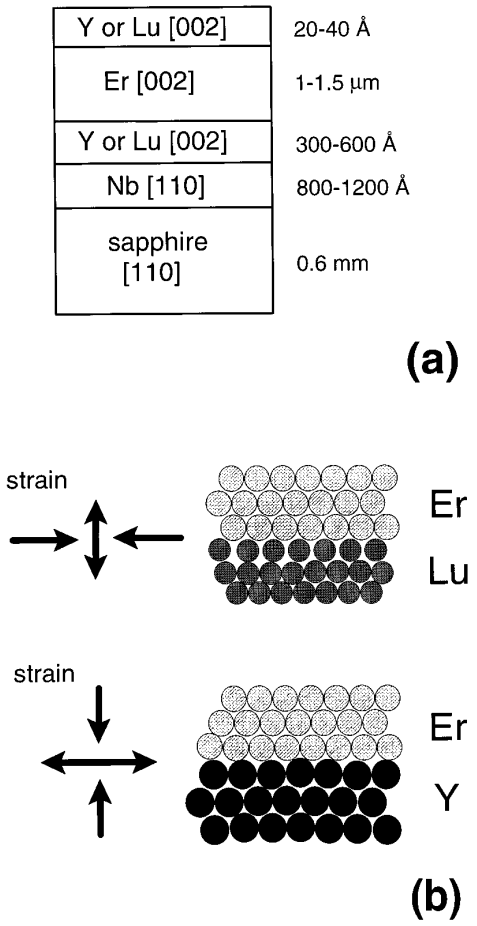

FIG. 1. (a) Structure of the Er/Y and Er/Lu films studied in the present experiment. (b) Schematic drawing of the strain in the Er films near the film-substrate interface.

random field problem.[8,9] So far as we are aware, there exists no complete description of an Er-like system, including all the effects noted above, which can be tested against our data.

Before turning to a discussion of the data, we review the magnetic structure of bulk erbium and of related thin films. Below its Néel temperature of $T_N \approx 86$ K, erbium forms an antiferromagnetic, incommensurate c-axis modulated structure (CAM) with no ordering of the moments in the a-b plane. The neutron and x-ray-diffraction patterns for this structure consist of magnetic satellites split symmetrically about each of the allowed chemical Bragg reflections (H,K,L), by $(0,0,\tau)$, where τ is the wave vector of the incommensurate magnetic structure. Near T_N, $\tau = 0.283$ in units of the reciprocal lattice $c^* = 2\pi/c (\approx 1.125\ \text{Å}^{-1})$ and increases as the temperature is lowered below T_N. In the CAM phase, the magnetic ordering also induces lattice modulations, which give rise to additional second- (and fourth-) order charge-scattering satellites along the $(0,0,L)$ direction.[7,10,11] At 52 K, there is a first-order phase transition to a cycloidal magnetic structure, in which the magnetic moments are mainly confined to the a-c plane.[12] The magnetic wave vector decreases with decreasing temperature below 52 K and exhibits a series of lock-in transitions to commensurate phases.[13,14] Neutron-scattering experiments[12] suggest that at intermediate temperatures the cycloidal structures are distorted by two-ion interactions of trigonal symmetry, making them wobble with a b-axis component of the moments supporting a slightly different wave vector than that of the a and c axes. Below about 18 K, there is a first-order transition to a ferromagnetic conical structure with wave vector $\tau = 5/21$, in which the moments are bunched around alternating a directions in a threefold symmetric pattern.[12] The transition to this phase is believed to be driven by changes in the magnetoelastic energy,[4] and is accompanied by large changes in the c- and a-axis lattice constants.

Characterizing the modifications to these structures which occur when Er is grown as a thin film or multilayer has been an active area of research.[5,6,15,16] Borchers *et al.*[6] originally discovered the suppression of the 5/21 cone phase in neutron-diffraction studies of Er films (up to $\sim 1.5\ \mu$m thick) deposited on Y substrates. In addition, they found a significant enhancement of the critical fields for the transition to the ferromagnetic phase, and showed that these effects follow the magnetostriction. Their modeling further revealed that the driving energy for the ferromagnetic transition varies linearly with strain, implying that strain effects are more important than even the artificial modulation in multilayers. These ideas have been amplified in neutron and magnetization studies of Er films deposited on Lu,[5] for Er thicknesses ranging from 400 to 9500 Å. In contrast to Er/Y, Er/Lu films of thickness greater than 1000–2000 Å do exhibit a low-temperature c-axis ferromagnetic phase similar to the 5/21 phase of the bulk. It is absent, however, in thinner Er/Lu films. A similar suppression has been found in Er/Lu multilayers[16] (for which the Er bilayer thickness is always less than 2000 Å) and in Er/Lu films grown on alloy substrates, for which the average a-axis lattice constants are matched to the bulk.[15] Our high-resolution x-ray-scattering results are largely consistent with these, and elucidate the nature of the ferrimagnetic phase which occurs at low temperature in thicker Er/Lu films.

In Sec. II of this paper we describe the experimental setup and the resonant x-ray magnetic scattering technique utilized in this work. Our results and a discussion are given in Sec. III and Sec. IV contains our conclusions.

II. THE EXPERIMENT

The thin-film samples studied here were grown by molecular-beam-epitaxy (MBE) techniques which have been described in detail elsewhere.[6,17] Figure 1(a) shows the general structure of the films. They were grown on $1.2\ \text{cm}^2 \times 0.6$ mm crystalline sapphire substrates with the [110] axis perpendicular to the growth plane. Reactivity between the rare-earth materials and the substrate was inhibited by a Nb[110] buffer layer of thickness 800–1200 Å, which was then followed by a 300–600 Å base layer of either Y or Lu. The nominal thicknesses of the erbium layers were 14 000 and 9500 Å for the Y and the Lu substrates, respectively; they were capped by a 20–40 Å Y or Lu layer. The crystal mosaics of the films were measured at their (0,0,2) reflections to be 0.25° (Y substrate) and 0.13° (Lu substrate) full width at half maximum (FWHM).

The x-ray-scattering experiments were performed on the bending magnet beamline X22C at the National Synchrotron Light Source. X22C is a doubly focused beamline equipped with a double-crystal Ge(111) monochromator and a

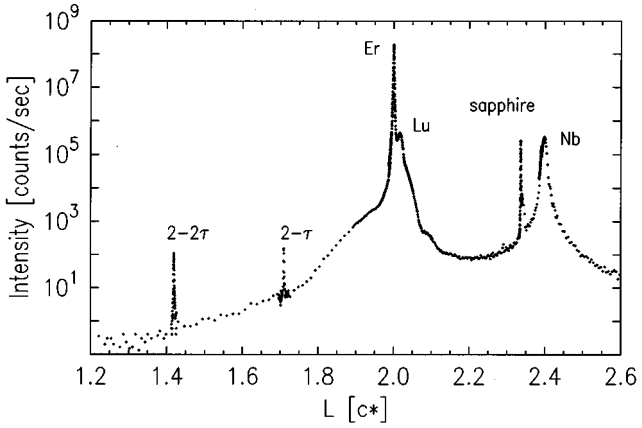

FIG. 2. Scan along the $(0,0,L)$ direction in reciprocal space for the 9500 Å Er film on a Lu substrate at $T=60$ K. The photon energy was tuned to the Er L_{III} absorption edge at $E=8.36$ keV.

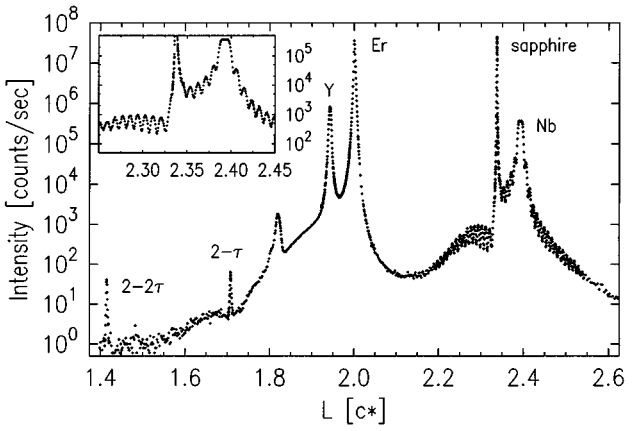

FIG. 3. Scan along the reciprocal $(0,0,L)$ direction at 60 K for the 14 000 Å Er film on a Y substrate measured at x-ray energy near the Er L_{III} edge ($E=8.36$ keV). The inset shows a magnification of the finite thickness interference fringes due to the Nb buffer layer.

Ge(111) analyzing crystal. In this configuration, X22C delivers approximately 10^{11} photons/sec in a ~ 1 mm^2 spot at an incident energy of 8 keV (5–10 eV bandwidth). The intensities of the incident and scattered beams were monitored using NaI scintillation counters. The momentum-transfer resolution was approximately 1×10^{-3}, 5×10^{-4}, and 2×10^{-2} Å^{-1} FWHM in the longitudinal, transverse, and out-of-scattering plane directions, respectively, as measured earlier at the (0,0,2) reflections of various bulk rare-earth single crystals.[7] The magnetic-scattering experiments were performed at the erbium L_{III} absorption edge at 8358 eV. Typical $(1/e)$ x-ray penetration depths at these energies are about 0.5 μm. The samples were mounted inside closed-cycle He refrigerators and the temperature monitored using Si-diode thermometers. The temperature stability during the course of a typical scan was about ± 20 mK.

It has been shown earlier that x-ray magnetic scattering in rare earths is resonantly enhanced when the incident photon energy is tuned near an L_{III} absorption edge.[18–20] In this case, the resonant cross section is described on the basis of electric dipole and quadrupole transitions between $2p$ core states and the $5d$ and $4f$ valence levels, respectively.[21] Specifically, the incident photon promotes a core electron to an unoccupied, symmetry-allowed valence state, which subsequently decays. The photon emitted in this decay corresponds to the elastic, magnetic scattering. The detailed energy and polarization dependences of these processes is well understood in the rare-earth metals.[18,21,22]

III. RESULTS AND DISCUSSION

A. Diffraction pattern along (0,0,L)

Figure 2 shows the scattered intensity for scans taken along the $(0,0,L)$ direction in reciprocal space near the Er(0,0,2) Bragg peak for the Er film deposited on Lu (Er/Lu). In addition to the closely spaced (0,0,2) reflections of Er and Lu, one sees the relatively broad (2,2,0) reflection of the Nb buffer layer and the extremely sharp (1,1,0) reflection of the sapphire substrate. This peak is offset slightly (by $\approx 0.05°$) from the $(0,0,L)$ direction of the Er film, indicating a small miscut between the sapphire substrate relative to the Er layer. The magnetic and charge scattering satellites at $(0,0,2-\tau)$ are seen clearly. On this scale, the magnetic satellite at $(0,0,2+\tau)$ is barely visible atop the high diffuse background scattering near the sapphire peak. The widths of the (0,0,2) and $(0,0,2-\tau)$ reflections for temperatures above 60 K were $\approx 1.6\times10^{-3}$ Å^{-1} FWHM and $<1.5\times10^{-3}$ Å^{-1}, respectively, in the longitudinal $(0,0,L)$ direction and $4-5\times10^{-3}$ Å^{-1} in the transverse $(H,H,0)$ direction for both peaks. (The latter is nearly ten times broader than the transverse resolution.) These widths correspond to lower limits for typical lengths $\xi\approx 2/\mathrm{FWHM}$ of the order of 1200–1400 Å in the longitudinal direction[23] and about 400 Å in the transverse direction. The $(0,0,4-\tau)$ and $(0,0,4-2\tau)$ reflections were also observed, both reduced in intensity by a factor ~ 4 relative to the corresponding satellites near (0,0,2).

A scan similar to that of Fig. 2 is shown for Er on a Y substrate (Er/Y) in Fig. 3. In this case, the charge scattering from the Y(0,0,2) reflection lies below that of the Er reflecting the difference in the Y and Lu lattice constants. The widths of the (0,0,2) and $(0,0,2-\tau)$ reflections for temperatures above 60 K were 3.4×10^{-3} and 2.8×10^{-3} Å^{-1}, respectively, in the longitudinal direction and 0.01 and 7×10^{-3} Å^{-1}, respectively, in the transverse direction. These correspond to lower limits for the lattice and magnetic correlation lengths of $\xi\approx 600-700$ Å along the c axis[23] and $\approx 200-300$ Å in the basal planes, which is reduced compared to Er/Lu. The broad peak near $L=1.824$ is powderlike when scanned in the transverse direction; its origin is unknown. The inset of Fig. 3 shows the interference fringes observed near the Nb (1,1,0) peak in detail. The spatial periodicity of these fringes was 9.9×10^{-3} Å^{-1}, indicating a Nb layer thickness of about 640 Å, which is slightly smaller than the ~ 800 Å thickness expected from the MBE growth conditions. Similar intensity oscillations were seen for the Er/Lu film along a direction slightly off the Er $(0,0,L)$ direction with a period of 1.07×10^{-2} Å^{-1}, which is close to that of the Er/Y film. Such finite thickness effects of Nb on sapphire have been studied in detail by Gibaud *et al.*[24] who developed a model in which the Nb layer is described by a two-dimensional network of domain walls, with an average separation of about 76 Å. Related studies have been carried out by Reimer *et al.*[25] and Miceli *et al.*[26] It is worth noting

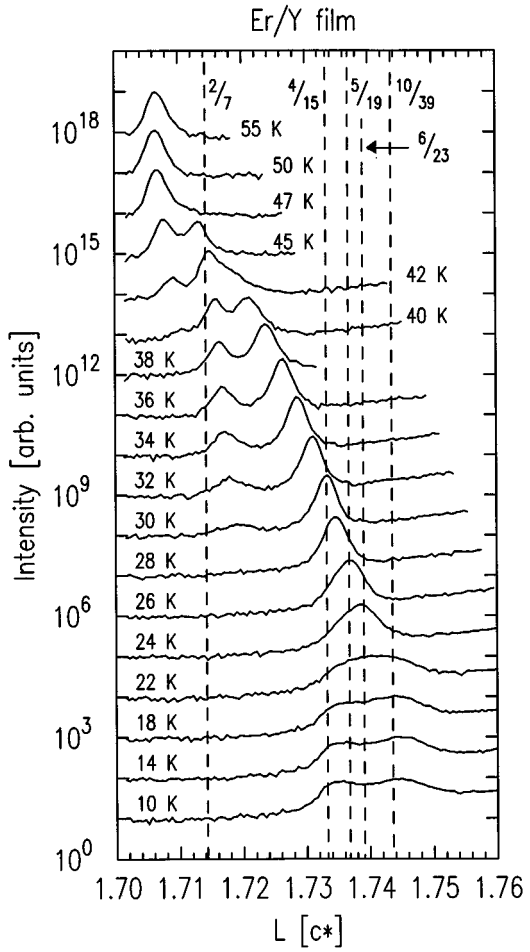

FIG. 4. Scans through the magnetic $(0,0,2-\tau)$ satellite of a 14 000 Å thick Er film on a Y substrate at various temperatures increasing from 10 K. Note the logarithmic scale on the intensity axis and that the curves have been shifted vertically for clarity. The values of L at some of the most pronounced lock-in transformations found in bulk Er (Ref. 14) are indicated by the vertical dashed lines.

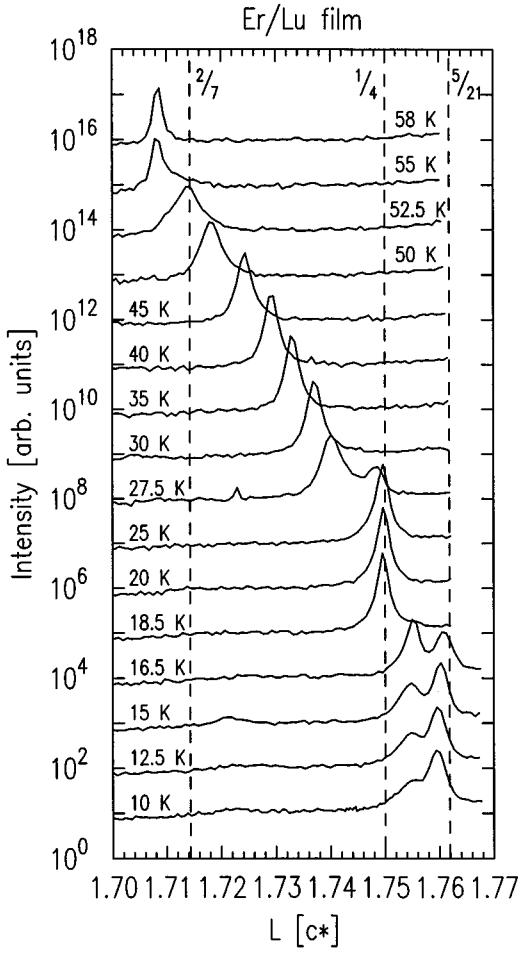

FIG. 5. The magnetic $(0,0,2-\tau)$ satellite of Er at various temperatures for a 9500 Å thick film on a Lu substrate measured on heating the sample from 10 K. (The curves are shifted vertically for clarity.) The vertical dashed lines show the positions of some lock-in transformations of bulk Er.

that the intensities of the sapphire substrate peaks are different in the scans shown in the two figures because the scan directions relative to the $(H,H,0)$ direction of sapphire were slightly different.

B. Temperature dependence of the magnetic wave vectors

The scattering at the magnetic $(0,0,2-\tau)$ reflection was monitored as a function of increasing and decreasing temperature for both films. Representative scans of the peaks are shown for selected, increasing temperatures in Figs. 4 and 5. It is clear from the figures that multiphase coexistence occurs throughout the magnetically ordered phases below 52 K, and especially at low temperatures, where the magnetic peaks are broad and overlapping. In order to extract the temperature dependence of the wave vectors, these data were fitted to sums of between one and three Lorentzian-squared or Gaussian line shapes, as needed, at each temperature. In particular, for the Er/Y film at low temperatures where the scattering was so broad as to make the identification of separate peaks difficult, starting wave vectors were first assigned to commensurate values found in bulk Er (Ref. 14) and subsequently allowed to float. These commensurate wave vectors are indicated by dashed lines in Figs. 4 and 5. Considering the freedom available in the fitting procedures, we do not claim that the deduced spectrum of wave vectors is unique, particularly for the Er/Y film at low temperature. However, in view of the simple interpretation given the results below, we believe that this analysis is worth presenting. It is also noteworthy that the c-axis magnetic correlation lengths deduced from the fitted peak widths at low temperatures were typically 300 Å in the Er/Y film and 600 Å in the Er/Lu film, both smaller than the c-axis correlation lengths of 600 and 1200 Å, respectively, at higher temperatures. The in-plane magnetic correlation lengths remained fixed between 200–300 Å in Er/Y and 400 Å in Er/Lu at all temperatures.

A summary of the temperature dependence of the wave vectors obtained by these procedures is shown for both samples in Fig. 6. For comparison, the temperature dependence of the magnetic wave vectors measured by x-ray scattering on a bulk Er sample is also shown. The qualitative behavior is similar in all three. In the c-axis modulated phase the magnetic wave vector increases with decreasing temperature from $\tau \approx 0.283$ at $T_N = 86$ K to ≈ 0.292 near 52 K. At $T \approx 52$ K in bulk, there is a transition to a cycloidal phase

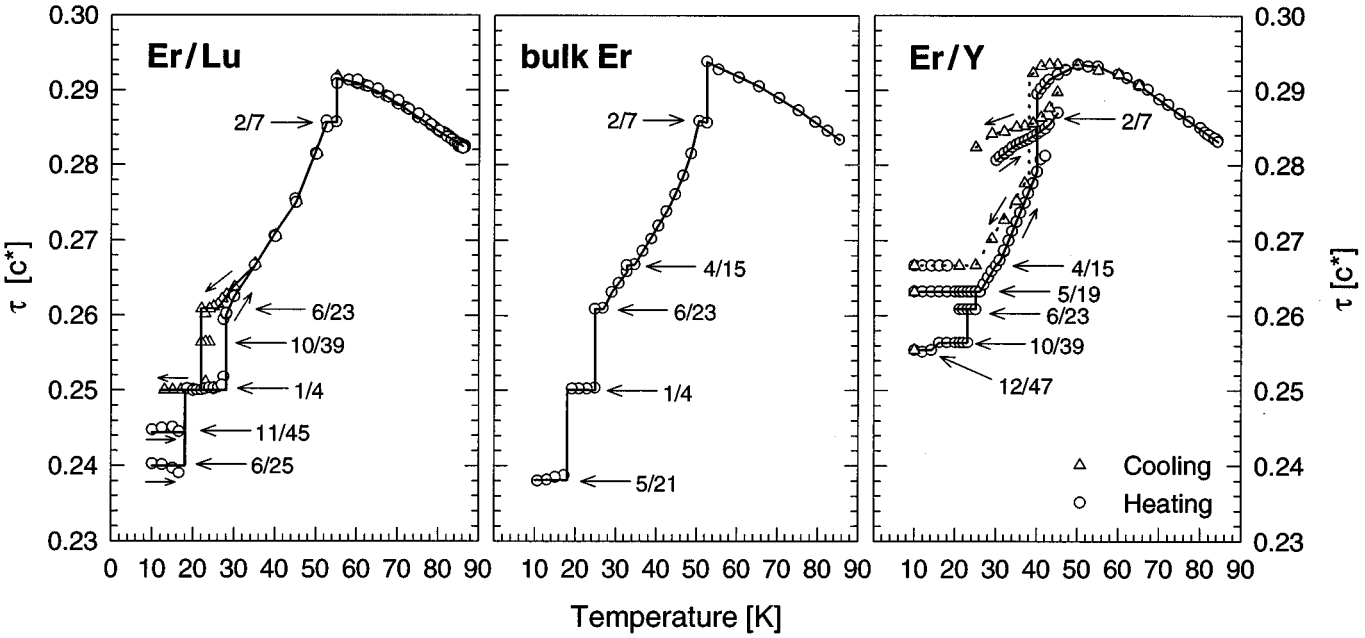

FIG. 6. Magnetic wave vector τ of Er as a function of temperature for an Er film on a Lu substrate (left), for bulk Er (middle), and for an Er film on a Y substrate (right). Small arrows are used to indicate the hysteresis found between measurements done on heating and cooling of the sample.

exhibiting both basal plane and c-axis components of the magnetic structure,[12] and which persists to 18 K. Although we have not carried out a detailed analysis of the magnetic intensities in the films, the similarity of the temperature dependence of the wave vectors to that in the bulk leads us to assume that cycloidal structures probably occur in the films also. Below 50 K, all three systems exhibit lock-in transformations to commensurate structures, often in coexistence with incommensurate or discommensurate structures (defined below). Hysteresis also occurs in all samples at the transitions to commensurate wave vectors, but it is especially marked in the films. The most striking differences between the two films are the complexity of the Er/Y diffraction pattern from 40 to 50 K, including marked hysteresis, and the absence of scattering at wave vectors equal or below 1/4 at low temperatures. In this regard, the behavior of the Er/Lu film is more like the bulk than is the Er/Y film, as has been reported earlier by Beach *et al.*[5]

In order to interpret the spectrum of observed wave vectors, we first recall the magnetic structure of bulk erbium.[12,14] In bulk, the lock-in wave vectors occurring below 52 K are[27] $\tau = 2/7$, 4/15, 6/23, 5/19, 1/4, and 5/21 (indicated by arrows in Fig. 6). Except for the 5/21 phase, which is believed to be a ferromagnetic spiral analogous to the conical phase of holmium,[12] the symmetry of these structures has a simple c-axis spin-slip description, namely, 2/7: (34), 4/15: (3444), 6/23: (344444), 5/19: (3444434444), and 1/4: (44), respectively. The sequence $(mn\cdots)$ gives the number of atomic planes for which the projected c-axis moment is first ''up,'' then ''down,'' etc. Thus, the 2/7 structure consists of a sequence of three planes with c-axis spins up, followed by four planes with c-axis spins down, etc. The term ''spin slip'' refers in this case to the absence of a spin within a quartet, to form a triplet. It is seen from the figure (and from earlier experiments) that the prevalent lock-in transitions in the bulk occur to simply commensurate structures with an integer ratio of quartets to triplets. For those structures, there is on average a single spacing separating triplets. Discommensurate structures, in contrast, have a disordered spin-slip distribution. Evidence of the existence of ordered (and disordered) triplet distributions is given in the bulk by the observation of lattice modulations along the c axis with wave vectors corresponding to the triplet periodicities.[14] In addition, the structures with an odd ratio of quartets to triplets are expected to be ferrimagnetic, which has been confirmed in bulk magnetization measurements.

Referring now to the data for the films, it is clear that most of the observed lock-in wave vectors correspond to simply commensurate spin-slip structures previously identified in the bulk. Reinforcing this view, the two new commensurate wave vectors extracted from the analysis of the films above 20 K, $\tau = 10/39$ and 12/47, also correspond to simple, ferrimagnetic spin-slip structures, namely, (4444444443) and (444444444443), respectively. From this perspective, the decrease of the magnetic wave vector with temperature proceeds via the decrease of the triplet density, from a quartet:triplet ratio of 1:1 near 50 K ($\tau = 2/7$) to 1:0 at 20 K ($\tau = 1/4$). The configurations which coexist at a given temperature depend upon the balance of the crystal-field and exchange interactions, including the trigonal coupling, and upon the strain distribution. Lock-in transitions to phases with ordered triplet distributions are presumably driven by the gain in crystal field or magnetoelastic energy derived from commensurability with the lattice. Otherwise, the triplet distribution is disordered. The effects of the strain seem most pronounced in the Er/Y film, as evidenced by the pervasive hysteresis, clustering of the wave vectors near 2/7 (without obvious locking),[28] multiphase coexistence, and by the absence of the 5/21 and 1/4 phases at low temperatures. It is worth recalling in this regard that the magnetic correlation

lengths are relatively short in the films. Indeed, the average triplet separation in the 12/47 phase of the Er/Y is comparable to the magnetic correlation length ($\sim$300 Å), corresponding to about one triplet in each domain along the c axis. This is consistent with our expectation that the strain distribution varies throughout the film, possibly inhomogeneously.

Although the temperature dependence of the magnetic wave vector exhibited by the Er/Lu film is more like the bulk than the Er/Y film, there are nevertheless fascinating differences from bulk behavior which we believe reflect the strain. For example, the magnetic wave vector of the Er/Lu film also fails to reach 5/21, and instead exhibits two-phase coexistence with wave vectors between 1/4 and 5/21, as shown in Figs. 5 and 6. We have assigned the new wave vectors the values 11/45 and 6/25, which is somewhat arbitrary in view of the broad longitudinal widths of the peaks.[29] It is important to note that in contrast to neutron scattering which measures the component of the magnetic structure perpendicular to the scattering plane, resonant magnetic x-ray scattering predominantly measures the component of the magnetic structure along the direction of the diffracted beam.[21,22] It is therefore, in principle, possible to measure two different wave vectors belonging to the same structure simultaneously if the magnetic structure has a different periodicity in the basal plane than along the c axis.[12] Then, the first component would give rise to an intensity varying proportional to $\cos^2\theta$, where 2θ is the scattering angle, and the intensity of the other component would vary as $\sin^2\theta$. Unfortunately, we did not measure the ratios of these intensities vs momentum transfer. Nevertheless, we believe that the presence of wave vectors near 11/45 and 6/25 in Er/Lu more likely arises from coexistence among separate domains, possibly with different degrees of strain.

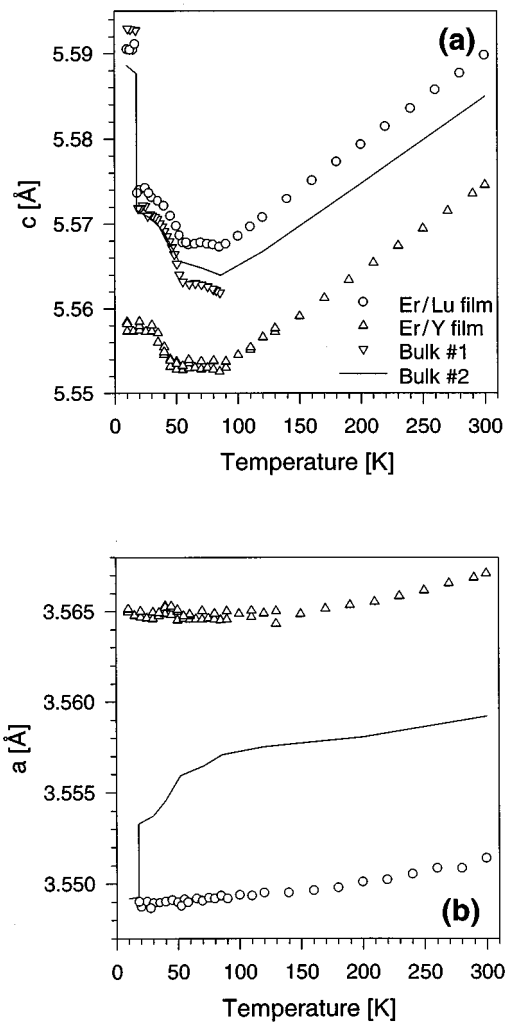

FIG. 7. (a) c-axis lattice constant vs temperature of thin Er film samples and bulk Er samples. Data for bulk sample No. 2 are taken from Ref. 31. (b) a-axis lattice constant vs temperature.

C. Temperature dependence of the a- and c-axis lattice constants

The temperature dependence of the average a- and c-axis lattice constants[30] for both films is shown in Fig. 7. These parameters were determined from measurements of the (0,0,2), (0,0,4), (1,0,4), and (2,0,4) peak positions at each temperature. Also shown are the values of c reported in earlier studies of bulk Er single crystals[7] (denoted bulk No. 1 in the figure caption). The solid lines show the lattice constant calculated from the bulk strain reported by Rhyne and Legvold[31] and adjusted to the room-temperature values found in Ref. 32. We emphasize that Fig. 7 shows only the average a- and c-axis lattice constants in the films (weighted by the x-ray absorption, which we neglect). It is likely that the atomic spacings and the microstructure of the crystal lattice vary throughout the film. One limiting model of the structure assumes that the Er lattice constants close to the film-substrate interface are strongly expanded (or contracted) to preserve epitaxy. It is even possible that they are modulated.[24,26] A second limit would have the epilayer relaxed to its average spacing by dislocations in the interface, and the remaining inhomogeneities attributed to stacking faults or other defects originating from the nucleation process in the growth of the interface. It is clear from Fig. 7 that the a-lattice constants of the films are clamped to their substrates, decreasing only slightly with decreasing temperatures, and that they otherwise exhibit no change at any of the magnetic phase transitions. This is quite different from the bulk behavior (solid line), for which the a and c lattice constants are nearly mirror opposites and plainly reflect the magnetic phase behavior. At room temperature, the bulk a lattice constants of Y and Lu are 3.648 and 3.505 Å, respectively, 2.5% larger and 1.5% smaller than bulk Er.[32] When deposited on Y in films 1 μm thick, the average Er a lattice constant is expanded by only 0.2% with respect to the bulk value in the paramagnetic phase, while on Lu, it is contracted by 0.2%. Thus, the Er lattice on Y suffers a greater distortion (near the interface) than on Lu, consistent with the reduced lattice correlation lengths.

The temperature dependences of the c-axis lattice constants of both thin films and the bulk are all qualitatively similar, varying nearly linearly with temperature from 300 K down to T_N. In the CAM phase, c is approximately constant in the films, but increases slightly with decreasing temperature in bulk. Below 52 K, in the cycloidal phase, c increases with decreasing temperature in all samples until about 18 K. At 18 K, the bulk c-axis lattice constant exhibits an abrupt increase at the transition from the cycloidal phase to the fer-

romagnetic cone phase with $\tau = 5/21$. A similar discontinuity is seen for Er/Lu, but is absent for Er/Y, which instead exhibits a plateau. It is interesting to note in this regard that at 10 K both c and a of the Er/Lu film are almost equal to the values found in bulk Er. Very recent studies[33] of an Er film grown on a Y-Lu alloy substrate show that when the in-plane lattice constants of the film become equal to those of the bulk, they also acquire the same wave vectors and probably the same magnetic structure. It seems clear from these observations that the magnetoelastic coupling, acting through the epitaxial strain and clamping introduced at the film/substrate interface, determine the magnetic phase behavior of the films.

It is interesting to speculate on the magnetic structures at low temperature. The discontinuities in the lattice constants of bulk Er at 18 K are associated with the transition to the conical phase.[4,34] In this phase, the single-ion anisotropy is strongly reduced and the trigonal anisotropy dominates,[12] favoring certain commensurate wave vectors like 5/21 as observed in the bulk. As noted above, the 5/21 wave vector is not observed in either film, but it is natural to infer that the presence of a discontinuity in the c-axis lattice constant of Er/Lu, and its absence in Er/Y, implies a conical phase in the former, but not in the latter. This interpretation is consistent with the magnetization curves measured for Er/Lu and Er/Y by Beach *et al.*[5] They found that the low-temperature magnetization of Er/Y saturates at a value of $\approx 0.4\ \mu_B$/atom at a field of ≈ 0.2 T, whereas the magnetization of Er/Lu jumps below 15–20 K to a value which exceeds the maximum obtainable ($\approx 0.53\ \mu_B$/atom) in a field of 0.2 T. According to mean-field calculations of the magnetic structure of Er by Jensen,[35] the magnetization observed in Er/Y is consistent with the ferrimagnetic moment of the 4/15 cycloidal structure (calculated to be $\approx 0.32\ \mu_B$/atom), whereas the low-temperature magnetization observed in Er/Lu may be produced only by the ferromagnetic cone (or by the 2/7 cycloidal structure, which is irrelevant at these temperatures).[36] A more extensive characterization of the intensities than has been performed here will be required before these cone phases may be regarded as experimentally established in the Er/Lu films.

D. c-axis strain profiles

On the basis of the observed magnetic and lattice correlation lengths, the average structure in the Er/Lu film may be thought of as consisting of blocks ~ 1200 Å long and ~ 400 Å across, supporting one or more magnetic domains (possibly with different wave vectors). Similarly, the average domain in the Er/Y film consists of a block 600 Å long and 200–400 Å across, and supporting one or more magnetic domains. This kind of scenario has been suggested for erbium films by Conover *et al.*,[15] although for much thinner films and smaller domains. It is clearly of great interest, if possible, to characterize the microstructure of the thin films more closely. Our approach here is to model a possible relaxation of the lattices as a function of distance from the substrate/film interfaces. Any strain distribution along the c axis should manifest itself, in principle, in the reflectivity profiles of the chemical Bragg reflections, especially in the wings, and may be inferred in part from curves like those shown in Figs. 2 and 3.

Although the full x-ray reflectivity profile from a layered structure is complicated to calculate, involving the lattice constants, strain and concentration profiles, and thicknesses and lattice symmetries of all the layers in the sandwich, it simplifies for wave vectors Q close to the Bragg peaks of one of the constituents. Therefore, to get a qualitative idea of the structure, we have modeled the scattering near the Er(0,0,2) reflection by considering a substrate consisting of n_s (0,0,1) planes of Y or Lu separated by a distance $d = c_s/2$ ($c_s = c_{\mathrm{Y}}$ or c_{Lu}, where the value of c_s is equal to the measured lattice constant at $T = 60$ K). On top of this we put n (0,0,1) planes of Er with plane separation $c/2$. If, as described, the in-plane a lattice constants of the Er/Y and Er/Lu films were clamped at the bulk values, this would require that the corresponding c-axis lattice constants are contracted or expanded, respectively, so as to approximately preserve the unit-cell volume. The specular reflectivity may then be calculated under the plausible assumption that the a- and c-axis lattice constants relax as a function of distance from the interface. Specifically, we assume that c decreases with depth below the film surface for Er/Y (corresponding to an increase in a) and that it increases for Er/Lu (corresponding to a decrease in a).

Examples of possible variations of c with depth below the film surface for Er/Y are shown in the lower inset of Fig. 8. They include (a) no variation, (b) tanh decrease, (c) linear decrease, and (d) quadratic decrease. The corresponding reflectivities plotted vs momentum transfer Q ($= Lc^*$) near the Er(0,0,2) reflection are shown on a logarithmic scale in the body of the figure, and on a linear scale in the upper inset. The calculated intensities were corrected for the Lorentz factor, scattering geometry and the absorption, and were convolved with the experimental resolution function (a Lorentzian squared with FWHM$\approx 1\times 10^{-3}$ Å^{-1}). The intensity shown earlier in Fig. 3, adjusted by a scale factor, is redrawn as a thick, solid line.[37] (Note that the curves in the inset have been adjusted to maximum intensity $= 1.0$ in order to make easier the comparison of the line shapes near the peak.)

Several features of Fig. 8 are notable. The measured reflectivity is much broader than that for the unstrained film, curve (a), and exhibits additional scattering on the high-L side of the (002) reflection. Allowing c to decrease with depth approaching the Er/Y interface (located at 1.4 μm in the lower inset) creates additional scattering on the high-L side, with relatively little change on the low-L side. This is in qualitative agreement with the data (thick line); however, neither the linear nor the quadratic curves fully captures the high-L Q dependence measured in this film. The oscillations seen in the calculated curve near the Y(0,0,2) reflection at $L = 1.944$ are due to the finite thickness of the Y layer, and were not observed—possibly as a result of steps or interdiffusion.

For the Er/Lu film, this modeling would imply an increase in c on approaching the Er/Lu interface (which, of course, implies a corresponding decrease in a). The upper inset of Fig. 9 shows the profile of the Er(0,0,2) reflection calculated for the three strain profiles shown in the lower inset. The measured peak (thick line) is only slightly broader than the calculated curve obtained for a strain-free Er layer [curve (a)]. The two other curves give only minor improvements in

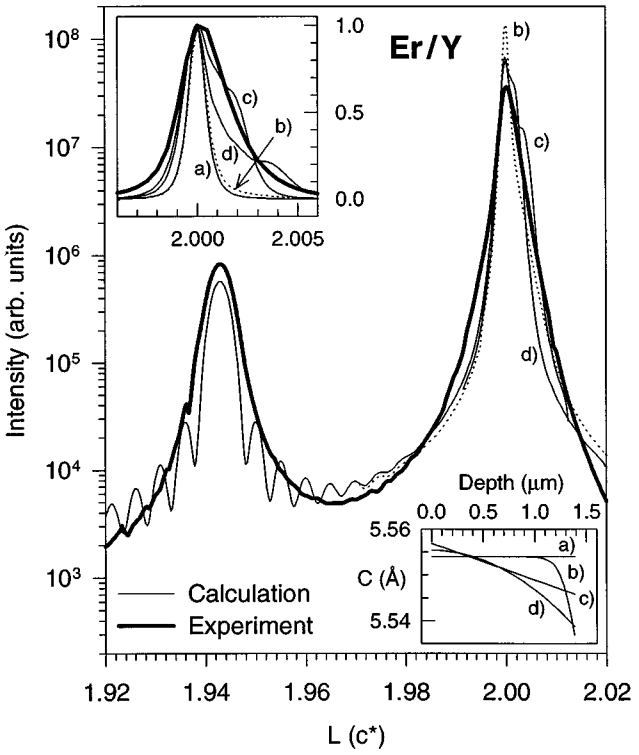

FIG. 8. Comparison between the experimental data at 60 K for the (0,0,2) reflection of Er on a Y substrate with the intensity calculated from a simple model with a varying lattice constant along the c axis. The model consists of $n=5000$ layers of Er (≈ 1.4 μm thickness) on top of $n_s=400$ layers of Y (≈ 1100 Å) and capped by 10 Y layers. The inset on the lower right shows four different c vs depth profiles $[(a)-(d)]$. The upper-left inset shows the longitudinal profile of the Er(0,0,2) reflection for the strain profiles $(a)-(d)$ on a linear scale. In this inset, the maximum intensity at $L=2.0$ has been scaled to 1.0 for all the curves in order to make the differences between the profiles clearer.

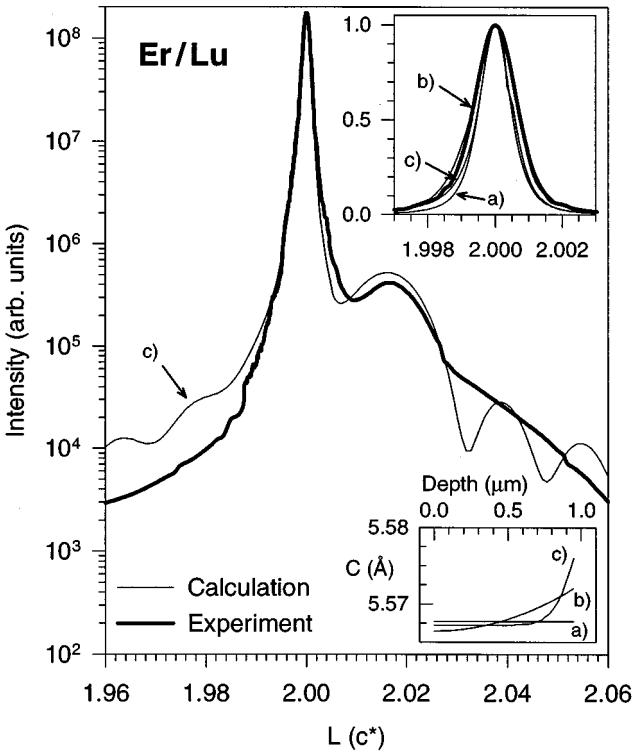

FIG. 9. Same legend as for Fig. 8 for the Er film on a Lu substrate. Here, the model system consists of $n=3400$ Er layers on top of $n_s=130$ Lu layers and capped by 10 Lu layers.

the agreement with the measured reflectivity. The strain profile (c) is used in the main body of Fig. 9, which also includes the broad Lu(0,0,2) reflection at $L=2.016$. This model fails to capture the low L dependence near $L=1.98$ and introduces finite-size oscillations which are not observed. It is worth noting that in both films the broad scattering lying beneath the Lu(0,0,2) and Y(0,0,2) charge peaks arise from the 20–40 Å caps on each film.

As can be seen from the above analysis, the main difference between the profiles of the Er(002) reflection in the two samples is that for Er/Lu the line shape is narrower and more symmetric, consistent with only weak variations in the layer separation, while for Er/Y the peak is much broader and asymmetric. The latter is consistent with a more distorted lattice, involving at least a contraction of the c-axis lattice constants, perhaps near the film-substrate interface as modeled here, and a partial relaxation closer to the outer film surface. Neither of the models is entirely satisfactory. A more detailed study of several chemical Bragg reflections, including off-axis reflections and the transverse reflectivity, is required before a more quantitative set of parameters may be deduced for the strain. Given the relatively short transverse lattice correlation lengths (large mosaics), it seems certain that the effects of the strain are even more pronounced within the basal planes. This latter behavior could be more consistent with alternative modeling of the strain inhomogeneity by stacking disorder distributed through the film.

E. Temperature dependence of the magnetic and charge scattering intensities near T_N

The temperature dependence of the integrated magnetic intensities of the $(0,0,2-\tau)$ peak in the CAM phases of the Er/Lu and Er/Y films is shown by the open circles in Figs. 10 and 11, respectively. We also studied the temperature dependence of the charge scattering at $(0,0,2-2\tau)$ in the Er/Lu film (triangles and squares in Fig. 10). Both peaks were studied at incident photon energies tuned near and far from the Er $L_{\rm III}$ absorption edge. For energies more than about 120 eV away from the edge, the magnetic peak was too weak to be observed. All of our data for the magnetic scattering was therefore obtained at resonance. Except for a scale factor, the temperature dependence of the charge-scattering peak was found to be independent of incident photon energy as shown in Fig. 10(b).

The universality classes appropriate for describing the paramagnetic-to-antiferromagnetic transitions of the bulk rare-earth metals remain controversial[7] and even less is known about thin films. Our earlier analysis of the scaling of the first-, second-, and fourth-order harmonic satellites of bulk Er (Ref. 7) showed that the intensities $I_{n\tau}$ $[=I(0,0,2-n\tau),\ n=1,2,4]$ of these peaks scale with the harmonic order n of the peak according to the predictions of mean-field theory, namely,

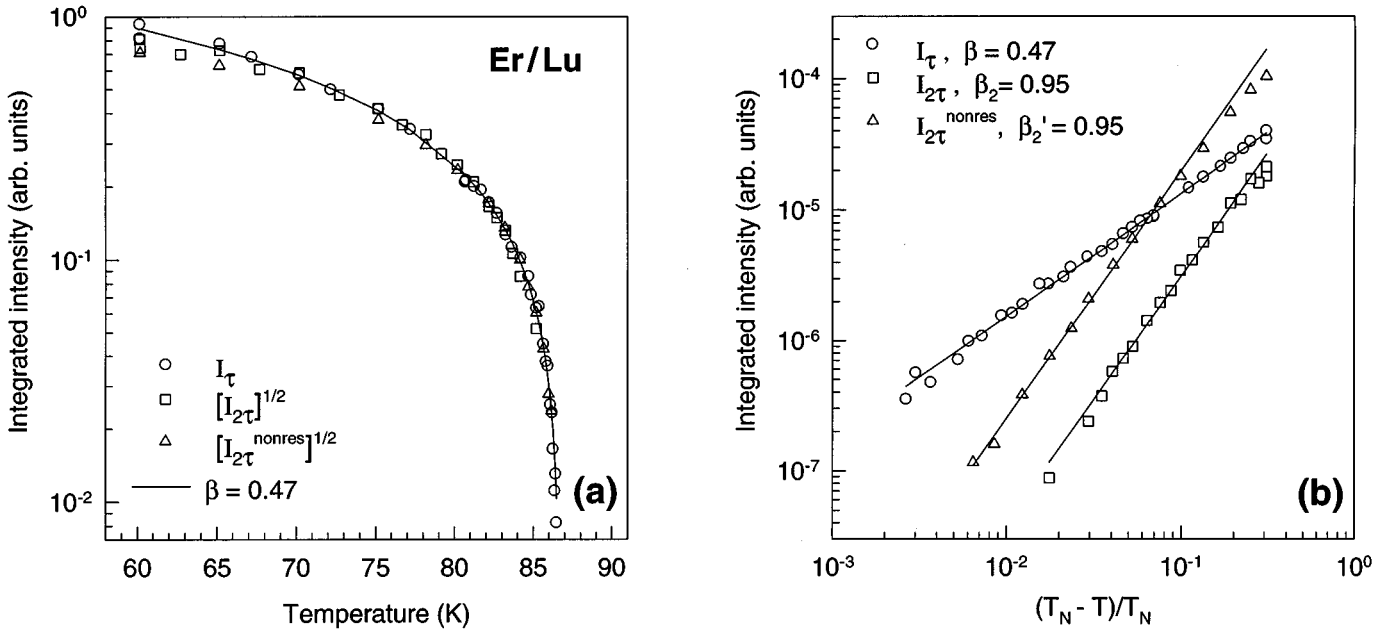

FIG. 10. (a) Integrated intensity I of the magnetic $(0,0,2-\tau)$ reflection (circles) and the charge-density-wave scattering at $(0,0,2-2\tau)$ (squares) measured with the x-ray energy near the $L_{\rm III}$ absorption edge of Er. Scaling of the first- and second-order satellites is obtained by raising the intensity of the second harmonic to a power 1/2, see Eq. (1). Also shown are data for $(0,0,2-2\tau)$ measured at $E=7.8$ keV (denoted ''nonres,'' triangular symbols). The result of a fit of I_τ to a power law, as discussed in the text, is shown as a solid line. (b) Integrated intensity I vs reduced temperature $(T_N-T)/T_N$ for the same data as in (a). Here, $T_N=86.7$ K. The solid lines show the best fits of the intensity data to power laws of the reduced temperature with critical exponents β and β_2.

$$I_{n\tau}\propto(I_\tau)^n\propto\left(\frac{T_N-T}{T_N}\right)^{2\beta_n}. \tag{1}$$

Here $\beta_n=n\beta$, where β is the critical exponent for the order parameter of the paramagnetic-antiferromagnetic phase transition. In bulk, we found $\beta\approx1/2$ for the CAM phases of both erbium and thulium.[7] Figure 10(a) shows that the dependence of I_τ and $(I_{2\tau})^{1/2}$ on temperature are very similar (after appropriate normalization). In order to confirm this agreement more quantitatively, the curves were fitted to the power-law behavior of Eq. (1). Figure 10(b) shows the measured intensities and best fits vs reduced temperature $(T_N-T)/T_N$ displayed on a log-log plot. The fitted values of the exponents are $\beta=\beta_1=0.47\pm0.03$ and $\beta_2=0.95\pm0.05=2\beta$, in agreement with the bulk values.[7]

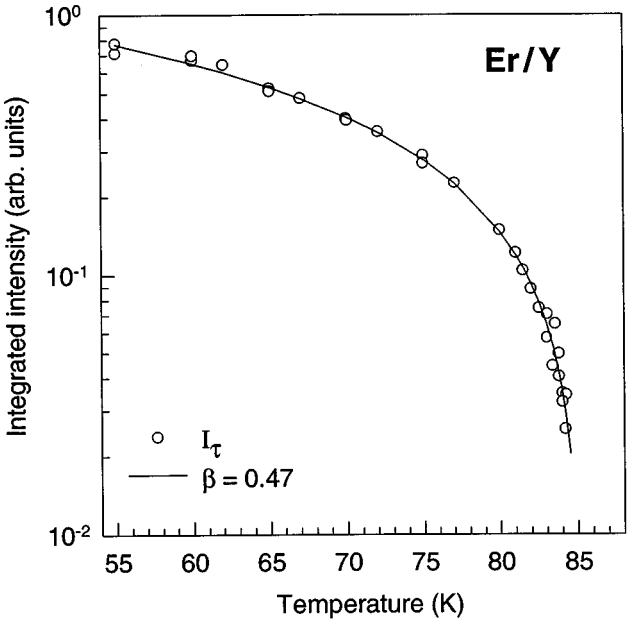

FIG. 11. Integrated intensity of the magnetic $(0,0,2-\tau)$ reflection of Er on a Y substrate. The solid line is a power law with critical exponent fixed at the value obtained from the Er/Lu film, $\beta=0.47$. For this film $T_N\approx85.1$ K.

The temperature dependence of the integrated magnetic intensity of the $(0,0,2-\tau)$ satellite is shown for the Er/Y film in Fig. 11. The lack of reliable data very close (<0.5 K) to the Néel temperature prevents an accurate determination of the critical behavior. However, as shown by the solid curve, a power-law description of the intensity I_τ using the same exponent $\beta=0.47$ found for Er/Lu (and putting $T_N=85.1$ K) gives satisfactory agreement with the measured data. Therefore, to within the available statistics, we find the same critical exponent β for the Er/Y and Er/Lu films as was found in bulk.

IV. CONCLUSIONS

We have carried out high-resolution x-ray-scattering studies of two Er films epitaxially grown on Y and Lu substrates. Although the magnetic phase diagrams of the films are qualitatively similar to that observed in bulk samples, the strain and clamping introduced at the interfaces alter the detailed temperature dependence of the magnetic structures, introducing multiphase coexistence and reducing the lattice and magnetic correlation lengths. Perhaps the most interesting result in this study is the suppression of the 5/21 bulk phase in both films, and its replacement in Er/Lu by two new magnetic

phases with wave vectors near 11/45 and 6/25. These wave vectors probably correspond to conical phases with structures similar to that of the 5/21 phase found in bulk Er. In this regard, it will be worth examining thin Er films grown on Lu-Y alloy substrates, where the average substrate lattice constants are matched to that of the bulk, in order to see whether the 5/21 phase reappears. The larger problem of disentangling the role of disorder on rare-earth magnetic phase behavior, as it is introduced through the interfacial strain, still remains. The complexity of these interfaces, and their dependence on growth conditions, continue to challenge systematic studies.

ACKNOWLEDGMENTS

It is a pleasure to acknowledge R. Du and A. Matheny who grew the Er/Y and Er/Lu thin films, respectively. We would like to thank J. Jensen for many helpful comments and suggestions and R. A. Cowley and J. Borchers for useful discussions. Work performed at Brookhaven is supported by the U.S. Department of Energy, Division of Materials Science under Contract No. DE-AC02-76CH00016. Work performed at the University of Illinois is supported by NSF DMR 94-24339. G.H. acknowledges the Research Council of Norway for partial financial support.

[1] C. F. Majkrzak, J. Kwo, M. Hong, Y. Yafet, D. Gibbs, C. L. Chien, and J. Bohr, Adv. Phys. **40**, 99 (1991).

[2] K. A. McEwen, in *Handbook on the Physics and Chemistry of Rare Earths*, edited by K. A. Gschneider and L. Eyring (North-Holland, Amsterdam, 1978), Vol. 1, p. 411.

[3] J. J. Rhyne, in *Handbook on the Physics and Chemistry of Rare Earths*, edited by K. A. Gschneider and L. Eyring (Elsevier, Amsterdam, 1988), Vol. 11, p. 293.

[4] J. Jensen and A. R. Macintosh, *Rare Earth Magnetism* (Clarendon Press, Oxford, 1991).

[5] R. S. Beach, J. A. Borchers, R. W. Erwin, J. J. Rhyne, A. Matheny, C. P. Flynn, and M. B. Salamon, J. Appl. Phys. **69**, 4535 (1991).

[6] J. A. Borchers, M. B. Salamon, R. W. Erwin, J. J. Rhyne, R. R. Du, and C. P. Flynn, Phys. Rev. B **43**, 3123 (1991); J. A. Borchers, M. B. Salamon, R. W. Erwin, J. J. Ryne, G. J. Nieuwenhuys, R. R. Du, C. P. Flynn, and R. S. Beach, *ibid.* **44**, 11 814 (1991).

[7] G. Helgesen, J. P. Hill, T. R. Thurston, and D. Gibbs, Phys. Rev. B **52**, 9446 (1995).

[8] T. Nattermann and J. Villain, Phase Transit. **11**, 5 (1988).

[9] D. Belanger, Phase Transit. **11**, 53 (1988).

[10] J. Bohr, D. Gibbs, and K. Huang, Phys. Rev. B **42**, 4322 (1990).

[11] K. Iwasa, N. Wakabayashi, T. Takabatake, H. Fujii, and T. Shigeoka, J. Phys. Soc. Jpn. **63**, 127 (1994).

[12] R. A. Cowley and J. Jensen, J. Phys., Condens. Matter **4**, 9673 (1992); J. Jensen and R. A. Cowley, Europhys. Lett. **21**, 705 (1993).

[13] M. Habenschuss, C. Stassis, S. K. Sinha, H. W. Deckman, and F. H. Spedding, Phys. Rev. B **10**, 1020 (1974).

[14] D. Gibbs, J. Bohr, J. D. Axe, D. E. Moncton, and K. L. D'Amico, Phys. Rev. B **34**, 8182 (1986).

[15] M. J. Conover, A. Kaldowsky, and C. P. Flynn, Phys. Rev. B **53**, R2938 (1996).

[16] J. A. Simpson, R. A. Cowley, D. F. McMorrow, M. R. Wells, R. C. C. Ward, C. J. Carlile, and M. A. Adams (unpublished).

[17] M. B. Salamon, S. Sinha, J. J. Rhyne, J. E. Cunningham, R. W. Erwin, J. Borchers, and C. P. Flynn, Phys. Rev. Lett. **56**, 259 (1986); R. W. Erwin, J. J. Rhyne, M. B. Salamon, J. Borchers, S. Sinha, R. Du, J. E. Cunningham, and C. P. Flynn, Phys. Rev. B **35**, 6808 (1987).

[18] D. Gibbs, G. Grübel, D. R. Harshman, E. D. Isaacs, D. B. McWhan, D. Mills, and C. Vettier, Phys. Rev. Lett. **61**, 1241 (1988); D. Gibbs, G. Grübel, D. R. Harshman, E. D. Isaacs, D. B. McWhan, D. Mills, and C. Vettier, Phys. Rev. B **43**, 5663 (1991).

[19] E. D. Isaacs, D. B. McWhan, C. Peters, G. E. Ice, D. P. Siddons, J. B. Hastings, C. Vettier, and O. Vogt, Phys. Rev. Lett. **62**, 1671 (1989).

[20] M. K. Sanyal, D. Gibbs, J. Bohr, and M. Wulff, Phys. Rev. B **49**, 1079 (1994).

[21] J. P. Hannon, G. T. Trammel, M. Blume, and D. Gibbs, Phys. Rev. Lett. **61**, 1245 (1988).

[22] J. P. Hill and D. F. McMorrow, Acta Crystallogr. Sec. A **52**, 236 (1996).

[23] A deconvolution of the longitudinal resolution function (assuming Lorentzian squared line shapes) increases the estimate of the longitudinal ξ to about 2000 Å for the Er/Lu film and $\xi \approx 800$ Å for the Er/Y film. The difference between the longitudinal widths of the $(0,0,2-\tau)$ and (0,0,2) peaks can be partly attributed to the variation in the width of the resolution function with wave-vector transfer.

[24] A. Gibaud, R. A. Cowley, D. F. McMorrow, R. C. C. Ward, and M. R. Wells, Phys. Rev. B **48**, 14463 (1993); A. Gibaud, D. F. McMorrow, and P. P. Swaddling, J. Phys., Condens. Matter **7**, 2645 (1995).

[25] P. M. Reimer, H. Zabel, C. P. Flynn, and J. Dura, Phys. Rev. B **45**, 11 426 (1992).

[26] P. F. Miceli and C. J. Palmstrom, Phys. Rev. B **51**, 5506 (1995).

[27] The existence of the 5/19 phase was inferred from the charge scattering corresponding to the spin-slip distribution (Ref. 14).

[28] It is worth noting here that the total shift of the magnetic wave vectors in the temperature range near $\tau = 2/7$ is comparable to, but exceeds, the fitted magnetic peak widths in that range.

[29] It is amusing to consider the possibility of a new variety of c-axis spin-slip structure for wave vectors $<1/4$, which, instead of being comprised of quartets and triplets, is comprised of quintets and quartets. Then, the wave vectors 5/21, 11/45, and 6/25 correspond to the c-axis sequences, 5/21: (44445)(44445), 11/45: (44444444445)(44444444445), and 6/25: (444445).

[30] F. J. Darnell, Phys. Rev. **132**, 1098 (1963).

[31] J. J. Rhyne and S. Legvold, Phys. Rev. **140**, A2143 (1965).

[32] K. A. Gschneider, in *Handbook on the Physics and Chemistry of Rare Earths*, edited by K. A. Gschneider and L. Eyring (Elsevier, Amsterdam, 1986), Vol. 8.

[33] G. Helgesen, M. Conover, D. Gibbs, C. P. Flynn, and M. B. Salamon (unpublished).

[34] S. Kawano, B. Lebeck, and N. Achiwa, J. Phys., Condens. Matter **5**, 1535 (1993).

[35] J. Jensen (private communication).

[36] According to Jensen's calculations (Ref. 35), the commensurate value 11/45 of the wave vector in the cone phase appears to be a realistic possibility. This structure has an effective period of 15 hexagonal layers (modulus 60°) which is relatively short in comparison with other commensurate structures with closely similar wave vectors. In contrast, the 6/25 cone structure has a much longer effective period (25 layers) than the 5/21 structure which has a seven-layer effective period. From this perspective, it is peculiar that the system chooses 6/25 over 5/21.

[37] It should be pointed out that the calculated reflectivity profile at $Q = Lc^*$ actually corresponds to the integrated intensity measured in a ''rocking-curve'' scan perpendicular to the $(0,0,L)$ direction in reciprocal space. This is only equivalent to the intensity measured in scans along the $(0,0,L)$ direction if the transverse resolution is broad enough to collect all the scattering at a particular value of L or if the transverse line shape and FWHM in $(H,H,0)$ scans are independent of L.